Biochimica et Biophysica Acta 1847 (2015) 1231–1239

Contents lists available at ScienceDirect

Biochimica et Biophysica Acta

journal homepage: www.elsevier.com/locate/bbabio

The two transmembrane helices of CcoP are sufficient for assembly of the *cbb*$_3$-type heme-copper oxygen reductase from *Vibrio cholerae*

Young O. Ahn [a], Hyun Ju Lee [c], Daniel Kaluka [b], Syun-Ru Yeh [b], Denis L. Rousseau [b], Pia Ädelroth [c], Robert B. Gennis [a,*]

[a] Department of Biochemistry, University of Illinois, 600 S. Mathews Street, Urbana, IL 61801, USA
[b] Department of Physiology and Biophysics, Albert Einstein College of Medicine, Bronx, New York 10461, USA
[c] Department of Biochemistry and Biophysics, Arrhenius Laboratories for Natural Sciences, Stockholm University, SE-106 91 Stockholm, Sweden

ARTICLE INFO

Article history:
Received 22 March 2015
Received in revised form 17 June 2015
Accepted 23 June 2015
Available online 25 June 2015

Classification:
Biological sciences
Biochemistry
Biophysics

Keywords:
Oxygen reductase
Membrane protein assembly
Bioenergetics
Vibrio cholerae
cbb$_3$

ABSTRACT

The C-family (*cbb*$_3$) of heme-copper oxygen reductases are proton-pumping enzymes terminating the aerobic respiratory chains of many bacteria, including a number of human pathogens. The most common form of these enzymes contains one copy each of 4 subunits encoded by the *ccoNOQP* operon. In the *cbb*$_3$ from *Rhodobacter capsulatus*, the enzyme is assembled in a stepwise manner, with an essential role played by an assembly protein CcoH. Importantly, it has been proposed that a transient interaction between the transmembrane domains of CcoP and CcoH is essential for assembly. Here, we test this proposal by showing that a genetically engineered form of *cbb*$_3$ from *Vibrio cholerae* (CcoNOQP^X) that lacks the hydrophilic domain of CcoP, where the two heme *c* moieties are present, is fully assembled and stable. Single-turnover kinetics of the reaction between the fully reduced CcoNOQP^X and O_2 are essentially the same as the wild type enzyme in oxidizing the 4 remaining redox-active sites. The enzyme retains approximately 10% of the steady state oxidase activity using the artificial electron donor TMPD, but has no activity using the physiological electron donor cytochrome c_4, since the docking site for this cytochrome is presumably located on the absent domain of CcoP. Residue E49 in the hydrophobic domain of CcoP is the entrance of the K^C-channel for proton input, and the E49A mutation in the truncated enzyme further reduces the steady state activity to less than 3%. Hence, the same proton channel is used by both the wild type and truncated enzymes.

1. Introduction

The vast majority of aerobic respiration by both prokaryotic and eukaryotic organisms is catalyzed by enzymes that are part of the superfamily of heme-copper oxidoreductases. This superfamily includes both heme-copper O_2 reductases (HCOs) as well as NO reductases (NORs). The HCOs are the terminal enzymes in the aerobic respiratory chains of most aerobic prokaryotes and virtually all eukaryotes. Of particular importance is that the HCOs are proton pumps that generate a proton motive force, thus conserving the substantial free energy available from the reaction in which O_2 is converted to water.

The HCOs have been categorized to 3 major subfamilies based on structural and phylogenetic analysis (A-, B- and C-families) [1]. The C-family HCOs, also known as cytochrome *cbb*$_3$, are most often expressed in bacteria growing under conditions of low aeration. The bacteria in which cytochrome *cbb*$_3$ plays a significant physiological role include a number of human pathogens, some of which rely solely on cytochrome *cbb*$_3$ for aerobic respiration. These enzymes, although capable of pumping 4 H^+/O_2 [2], under some circumstances pump protons less efficiently in vivo [3].

The C-family HCOs share one homologous subunit with other heme-copper O_2 reductases [1,4], often referred to as subunit I or, in the case of cytochrome *cbb*$_3$, CcoN. As in all the HCOs, subunit I contains a low spin heme as well as the heme-copper binuclear active site where O_2 binds and is reduced to water. In the case of the *cbb*$_3$-type oxygen reductases (C-family enzymes), the low spin and high spin hemes are both heme B (protoheme IX). The active-site heme in all other HCOs (A-family and B-family) appears to be variants of either heme O or heme A. Subunit I in all HCOs contains channels leading to the heme-copper active site for the delivery of O_2 and for protons [3]. There is only one proton input channel for the C-family HCOs (the K^C-channel) [4], whereas the A-family HCOs, which include the mitochondrial cytochrome *aa*$_3$, have two proton-delivery channels (K-channel and D-channel) [3].

With one exception, all the biochemically characterized C-family HCOs have four subunits, CcoN, CcoO, CcoP and CcoQ, encoded by the *ccoNOQP* operon. These include the enzymes isolated from *Pseudomonas stutzeri* [4,5], *Rhodobacter sphaeroides* [6], *Rhodobacter capsulatus* [7],

Abbreviations: TMPD, N,N,N′,N′-tetramethyl-p-phenylenediamine; PMS, phenazine methosulphate; HCO, heme-copper oxygen reductase; DDM, n-dodecyl β-d-maltoside.

* Corresponding author.
E-mail address: r-gennis@illinois.edu (R.B. Gennis).

http://dx.doi.org/10.1016/j.bbabio.2015.06.013
0005-2728/

Paracoccus denitrificans [8], *Bradyrhizobium japonicum* [9], *Rhodothermus marinus* [10] and *Vibrio cholerae* [11]. The exception is one of the two cbb_3-type HCOs from *P. stutzeri* [5], in which the CcoQ subunit is absent. The role of the CcoQ subunit is not clear, but it may be important for enzyme stability in at least some cases [12,13]. The X-ray structure of one of the variants of cytochrome cbb_3 from *P. stutzeri* has been determined [4], showing how these subunits are arranged in the complex (Fig. 1).

Whereas CcoN, with 12 transmembrane helices, is homologous to subunit I in the A- and B-family HCOs, the CcoO, CcoP and CcoQ subunits share no similarity with subunits found in A- or B-family HCOs. Subunits CcoO, CcoP and CcoQ each contain at least one but no more than two transmembrane helices. CcoO contains a hydrophilic domain with one heme *c*, which is the immediate electron donor to the low spin heme *b*. CcoP in most cases contains two hemes *c*, but in some enzymes one or three, which provide the "electron wire" directing electrons from periplasmic electron donors to the heme *c* in CcoO. CcoQ is not required for either assembly or catalytic activity of the cytochromes cbb_3 from either *R. sphaeroides* [14] or from *B. japonicum* [15]. However, CcoQ has been shown to be important for stabilizing the interaction between CcoP and the core complex CcoNO in the enzyme from *R. capsulatus* [12].

A number of bacterial genomes encode putative variants of cytochrome cbb_3, which include only CcoN and CcoO, presumably representing a minimal 2-subunit core required for function [16]. This is consistent with observations that subcomplexes of the cytochromes cbb_3 from *B. japonicum* and from *P. denitrificans* that contain only CcoN and CcoO retain at least a small amount of TMPD oxidase activity [15,17]. On the other hand, the assembly of the CcoNOQP complex as an active enzyme requires the CcoP subunit [15,18,19].

Just downstream of the *ccoNOQP* operon in many bacterial genomes is a second gene cluster, *ccoGHIS*, which encodes proteins required for the assembly of the cytochrome cbb_3 [7,12,15,18,20,21]. CcoG, CcoI and CcoS all play roles in the maturation of the CcoN subunit of cytochrome cbb_3 [22], and are proposed to be either necessary for or assist in the insertion of the two hemes *b* (CcoS) [20] or Cu_B (CcoI, CcoG) [20–22]. CcoH appears to be necessary for the assembly of the final active CcoNOQP complex from two pre-assembled complexes, CcoNO and CcoQP [18,22]. Crosslinking and immunoprecipitation studies show that CcoH interacts with CcoP primarily via interactions with the single transmembrane span of CcoH [23]. A second interaction of CcoH with the CcoNO complex has also been shown [23] as well as an interaction with the mature CcoNOQP complex [5]. Hence, it is possible that CcoH is an authentic subunit of the mature enzyme, but is readily lost upon purification [23]. In the absence of CcoH, neither the active cytochrome cbb_3 nor the CcoNO or CcoQP subcomplexes can be detected in the membranes of *R. capsulatus* [23].

The current work tests the model that the assembly of cytochrome cbb_3 might only require interactions between CcoH with the transmembrane domain of CcoP by truncating the C-terminal hydrophilic domain of CcoP from the cytochrome cbb_3 from *V. cholerae*. The results confirm that the truncated CcoNOQP^X is assembled and is stable, and retains about 10% of the TMPD oxidase activity of the wild type enzyme.

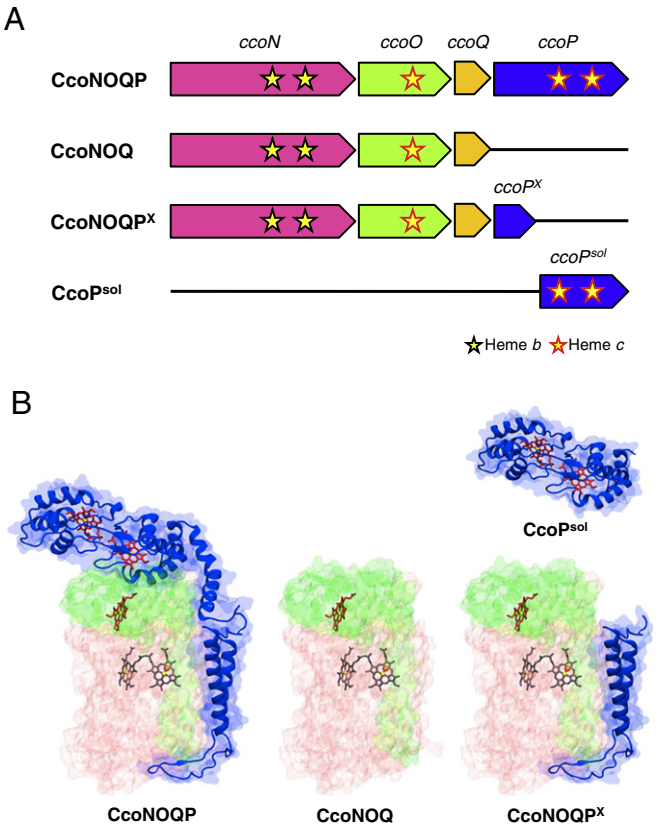

Fig. 1. The structure of modified versions of cytochrome cbb_3 from *Vibrio cholerae* (A) The *ccoNOQP* operon of *V. cholerae* and engineered variants used in this work. (B) The structures corresponding to the operons shown in Panel (A) based on the structure of the enzyme from *P. stutzeri* (PDB ID: 3MK7) [4]. Subunit I (CcoN), subunit II (CcoO), subunit III (CcoP) and subunit IV (CcoQ) are shown in pink, green, blue and orange, respectively. CcoP^X and CcoP^{Sol} in ribbon structure represent the transmembrane helices of the CcoP and the soluble domain of the CcoP subunit, respectively. It is assumed that CcoQ is an integral part of the complex, though this has not yet been demonstrated.

2. Material and methods

2.1. Site-directed mutagenesis and purification of cbb_3 oxidase

The mutations were constructed using QuikChange site-directed mutagenesis kits from Stratagene. DNA oligonucleotides were synthesized at Integrated DNA Technologies. Sequence verification of the mutagenesis product was performed at the Biotechnology Center at the University of Illinois at Urbana-Champaign. The expression, purification, and characterization of the *V. cholerae* cbb_3 wild type and mutants was performed as previously described [11,33]. Briefly, *V. cholerae* (0395N1) cells were grown at 37 °C and 220 rpm in LB media with 100 μg/L ampicillin (Fisher Biotech) and 100 μg/L streptomycin (Sigma). The expression of protein was induced with 0.2% L-(+)-arabinose (Sigma). The membranes were collected at 40,000 rpm by ultracentrifugation from cell lysate and solubilized with 0.5% dodecyl β-D-maltoside (Anatrace). The protein was then purified using a Ni-NTA affinity column (Qiagen, CA).

2.2. Thermal stability measurements

Dynamic light scattering (DLS) techniques were applied to measure the size distribution (Z-average size) of enzymes while varying temperatures (DLS, Malvern Zetasizer Nano ZS90, Malvern Instruments Ltd., U.K.). The Z-average size is a parameter also known as the cumulants mean as the harmonic intensity averaged particle diameter. Increase in Z-average size with DLS exhibits increase in the size of enzymes resulting from the formation of aggregate enzymes due to protein denaturation. 3 individual DLS Data points were collected at each 2.5 °C increment between 4 °C and 65 °C, and the experiments were repeated twice for each sample. For the measurement, 5 μM of the cbb_3 variants were prepared in 50 mM sodium phosphate buffer, 100 mM NaCl and 0.05% dodecyl β-D-maltoside (DDM) at pH 8.0.

2.3. Reconstitution of the *V. cholerae* cbb_3 enzyme into phospholipid vesicles

Cytochrome *c* oxidase vesicles were produced by reconstituting the *V. cholerae* cbb_3 into small unilamellar phospholipid vesicles, and detergent was removed by Bio-beads (BioRad) essentially as in [34]. Asolectin (Sigma) (80 mg/mL) was mixed with 2% cholic acid in 100 mM Hepes at pH 7.4 and then sonicated using a model W-375

sonicator (Heat Systems-Ultrasonics, Inc.) on ice under a stream of argon gas. The cbb_3 oxidase was added to the sonicated lipid/cholate mixture to a final concentration of 1 μM. Bio-beads (66 mg/mL) were added to the enzyme mixture every 30 min for 4 h at 4 °C with agitation. After adding 100 mM Hepes buffer (0.5 mL per mL of mix), bio-beads were added every 30 min for another 3 h (133 mg/mL during the first 2 h and 266 mg/mL during the last hour) at room temperature. The proteoliposomes were dialyzed overnight against 60 mM KCl.

2.4. Isolation and characterization of soluble CcoP ($CcoP^{sol}$)

To amplify the periplasmic domain of *ccoP* gene (141–326 aa), forward and reverse primers were designed to introduce HindIII and BamHI sites, respectively, which facilitated cloning into the expression vector pET-17b to yield a new construct, pETsolCcoP(Ap^r): 5′-CCCAAG CTTCAGACCACTAACTTACGCGAAATCC-3′ (forward primer) and 5′-CGGGATCCTTACTTATTCTCTGAGTTGCTTAAGCTC-3′ (reverse primer). The modified signal peptide of cytochrome c_{550} from *Thiobacillus versutus* was introduced before N-terminal of the operon $ccoP^{sol}$ and expressed successfully in *E. coli* BL21(DE3), which also contains pEC86(Cm^r), yielding a soluble CcoP. DNA sequencing (Biotechnology Center at the University of Illinois at Urbana Champaign) confirmed that the insert was identical in sequence to the periplasmic domain of CcoP. Condition of cell growth and enzyme expression were previously described [26]. The cells were grown in 1 L of LB medium, supplemented with 100 μg/mL ampicillin and 30 μg/mL chloramphenicol, in a 2.8 L Fernbach flask at 37 °C and 100 rpm, and the gene expression is induced with 1 mM ITPG when OD_{600} is about 0.6–1.0. The cells were harvested at 4 °C by centrifugation at 8000 ×*g* for 10 min. The soluble extract was prepared as previously described in [26]. Crude extract was loaded onto CM-52 cellulose column (Whatman) preequilibrated with 25 mM Tris–HCl buffer (pH 7.5) and the adsorbed proteins from column were eluted with linear gradient of NaCl from 0 to 1 M. Partially purified protein fractions were purified further by the DEAE-Sepharose column as described above. Purified fractions of the $CcoP^{sol}$ were concentrated (200–300 μM) using concentrator (Amicon) with YM-10 membranes and stored at −80 °C after flash-frozen in liquid nitrogen.

2.5. Steady-state activity

Steady-state activity was measured with a YSI model 53 oxygen monitor. For the TMPD oxidase activity, the reaction mixture contained buffer (50 mM sodium phosphate, 100 mM NaCl and 0.05% DDM at pH 6.5), 10 mM ascorbate and 500 μM TMPD as previously described [25]. The pH dependence of the TMPD enzyme activity displays only data between pH 6.5 and pH 9.0 since below pH 6.5 the enzyme activity was decreased. For the measurement of cytochrome *c* enzyme activity, the cytochrome cbb_3 wild type and the $NOQP^X$ were tested respectively using 20 mM ascorbate in combination with either 50 μM of the *V. cholerae* cytochrome c_4 or 50 μM of the $CcoP^{sol}$ under the same buffer conditions as for the TMPD enzyme activity assay.

2.6. Resonance Raman spectroscopy

The resonance Raman spectra were obtained as previously described [35]. Briefly, the 413.1 nm excitation from a Kr ion laser (Spectra-Physics, Mountain View, CA) was focused to an ~30 μm spot on the spinning quartz cell rotating at ~1000 rpm. The scattered light, collected at a right angle to the incident laser beam, was focused on the 100 μm-wide entrance slit of a 1.25 m Spex spectrometer equipped with a 1200 groove/mm grating (Bausch & Lomb, Analytical Systems Division, Rochester, NY), where it was dispersed and then detected by a liquid nitrogen-cooled CCD detector (Princeton Instruments, Trenton, NJ). A holographic notch filter (Kaiser Optical Systems, Ann Arbor, MI) was used to remove the laser line. The Raman shifts were calibrated with indene. The concentration of enzyme was 50 μM. The laser powers used for all Raman measurements are indicated in the captions.

2.7. CO-flash-photolysis

The enzyme samples were prepared as previously described [25]. Briefly, the enzyme at a concentration of ~5 μM was transferred to a modified anaerobic cuvette and the atmosphere was exchanged to N_2 on a vacuum line. The enzyme was completely reduced by addition of 2 mM ascorbate and 2 μM phenazine methosulphate (PMS). Then, N_2 was exchanged for CO so that anaerobic incubation in CO results in formation of fully reduced CO-bound cbb_3 oxidase. The CO-ligand was photolyzed by a 10 ns laser flash at 532 nm (Brilliant B, Quantel), followed by detection of absorbance changes by an apparatus from Applied Photophysics [36].

2.8. Flow-flash measurements

Flow-flash measurements were performed using a modified stopped-flow apparatus (Applied Photophysics, Surrey, U.K.) and data analyzed as described in [24,25]. The enzyme solution (50 mM Hepes, 50 mM KCl, 0.03% DDM and 50 μM EDTA at pH 7.4) was rapidly mixed in a 1:5 ratio with an O_2-saturated buffer, and the reaction with O_2 was initiated by flash photolysis of the CO-enzyme complex approximately 200 ms after mixing. The kinetics was monitored optically as absorbance differences at single wavelengths.

3. Results

Fig. 1 shows the gene constructs that were examined in this work. The wild type enzyme from *V. cholerae* is encoded by the *ccoNOQP* operon (Fig. 1A) which yields the 4-subunit CcoNOQP cytochrome cbb_3 (Fig. 1B). For the current work, all the constructs included a His-tag at the C-terminus of CcoN to facilitate purification. The CcoP subunit has two transmembrane helices and large hydrophilic domain which lies on the top of the enzyme (facing the periplasm). CcoO has a single transmembrane domain and a hydrophilic domain that is sandwiched between CcoN and CcoP. When the *ccoP* gene is deleted from the operon, expression of the remaining *ccoNOQ* does not result in any detectable enzyme in the membranes of *V. cholerae* (Table 1). The hydrophilic domain of CcoP is connected to the transmembrane helices by a long helical linker from Q89 to A136 [4]. Stop codons were inserted either just after Q89 or after Q109, and the operons $ccoNOQP^{89X}$ and $ccoNOQP^{109X}$ were expressed. Each yielded truncated variants of cytochrome cbb_3 in yields comparable to the wild type enzyme, and the truncated enzymes, $CcoNOQP^{89X}$ and $CcoNOQP^{109X}$, were stable and could be purified and examined (Table 1). Since the two truncated versions appeared to be identical, only the version truncated after Q89 was examined in detail. This will be referred to either as the truncated

Table 1
Comparison of the properties of the wild type and mutant variants of cytochrome cbb_3 from *V. cholerae*.

Mutants	Turnover % (e^-/s cbb_3)	Assembly
WT	100 (200 e^-/s)	+
$E49^{III}A^*$	10	+
$CcoNOQP^{89X}$ (his^I)	9	+
$CcoNOQP^{89X}$ (his^{III})	15	+
$CcoNOQP^{109X}$ (his^I)	8	+
$CcoNOQP^{89X}$-$E49^{III}A$	<3	+
CcoNO	N/D	−

All residue numbers are for cytochrome cbb_3 from *V. cholerae*. The superscripts indicate mutations in Subunit I (CcoN) or Subunit III (CcoP); "his", histidine tag; "*", previously reported in [25]. The assembly of the cytochrome cbb_3 are indicated as "+", normal assembly; "−" no enzyme complex obtained after purification; "ND", not determined.

enzyme or CcoNOQP^X. It is evident that the hydrophilic domain of CcoP is not required for the assembly or stability of cytochrome *cbb*$_3$.

3.1. Subunit and heme analysis

Fig. 2 shows the SDS-PAGE analysis of the purified wild type and CcoNOQP^X. When stained with Coomassie blue, CcoN, CcoO and CcoP are apparent in the wild type enzyme at 57 kDa, 23 kDa and 34 kDa (Fig. 2A). The small subunit CcoQ is not observed. In contrast, the band corresponding to CcoP is missing from the truncated version of the enzyme. Similarly, when the bands are visualized using a stain for the covalently bound heme *c*, both CcoO and CcoP are evident in the lane with the wild type enzyme, but only CcoO is in the lane with the truncated enzyme (Fig. 2B). The remaining transmembrane fragment is expected to be present in the CcoNOQP^X enzyme having a molecular weight of 9.7 kDa and is not observed in the gel. In order to verify the presence of the small, hydrophobic fragment of CcoP^{89X} in the preparation of CcoNOQP^X, the His-tag was moved from subunit CcoN to the C-terminus of CcoP^X, following residue W88. The CcoNOQP^{89His} enzyme was expressed and purified using the Ni-affinity resin (Table 1). The isolated enzyme contained CcoO and CcoN, demonstrating that the transmembrane domain of the CcoP^X remains attached to the truncated cytochrome *cbb*$_3$.

A pyridine hemochrome analysis was performed on the preparations of both the wild type and truncated enzyme to quantify the heme contents. The results showed the expected heme *b*:heme *c* ratio of 2:3 for the wild type enzyme, and a heme *b*:heme *c* ratio of 2:1 for the truncated cytochrome *cbb*$_3$. The data indicate the absence of the hemes *c* in CcoP due to the truncation, consistent with the lack of CO binding to the hemes *c* in CcoP shown in the UV–visible heme spectra of the truncated enzyme (see Fig. 2C and D).

3.2. Thermal stability

Dynamic light scattering (DLS) was used to monitor thermal denaturation of the proteins as the temperature was increased from 4 °C to 65 °C. Protein denaturation results in aggregation which is observed by DLS as an increase in the "Z-average" parameter. Fig. 3 displays that the Z-average starts to increase at ~42 °C for both the wild type and CcoNOQP^X indicating that the thermal stability of the truncated cytochrome *cbb*$_3$ is similar to that of the wild type.

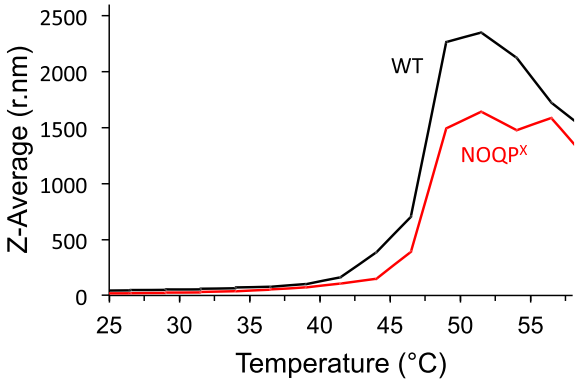

Fig. 3. Thermal stability of the truncated enzyme (CcoNOQPX) shown in red, compared to the wild type cytochrome *cbb*$_3$, shown in black. The size distribution profile (Z-average size) of enzymes was determined using dynamic light scattering (DLS) technique while varying the temperature. The traces have been shown from 25 to 57 °C for better comparison.

3.3. Steady state kinetics

The steady state oxygen reductase assay was performed using the artificial electron donor TMPD. The wild type enzyme has a turnover of about 200 e^-/s and the CcoNOQP^X enzyme retains about 9% of this activity (18 e^-/s) (Table 1). TMPD is often used as a reductant for cytochrome *c*-dependent enzymes, and the truncated cytochrome *cbb*$_3$ still retains a cytochrome *c* in the remaining CcoO subunit. The low activity is likely due to the fact that the heme *c* in the CcoO subunit is buried within the subunit and not readily accessed by the TMPD molecules in solution. The activity of the truncated enzyme (CcoNOQP^{89His}) isolated by the His-tag located at the C-terminus of CcoP^X has higher specific activity, about 15% of the wild type value (Table 1), suggesting that perhaps there is a fraction of the preparation of the truncated enzyme isolated by the His-tag on CcoN which is inactive due to the loss of the transmembrane helices of CcoP subunit from the truncated CcoNOQP^X.

The K^C-proton channel that is required to deliver protons to the active site for catalytic function has its entrance, E49, within the remaining hydrophobic domain of CcoP^X [24,25]. Mutation of this residue (E49A) in the full-length *V. cholerae* cytochrome *cbb*$_3$ reduces the TMPD oxidase activity to 10% of the wild type value [24,25]. The same mutation, E49A, in the CcoNOQP^X variant reduces the activity from 9% to less than 3% of the wild type activity (Table 1). The data suggest that the proton input

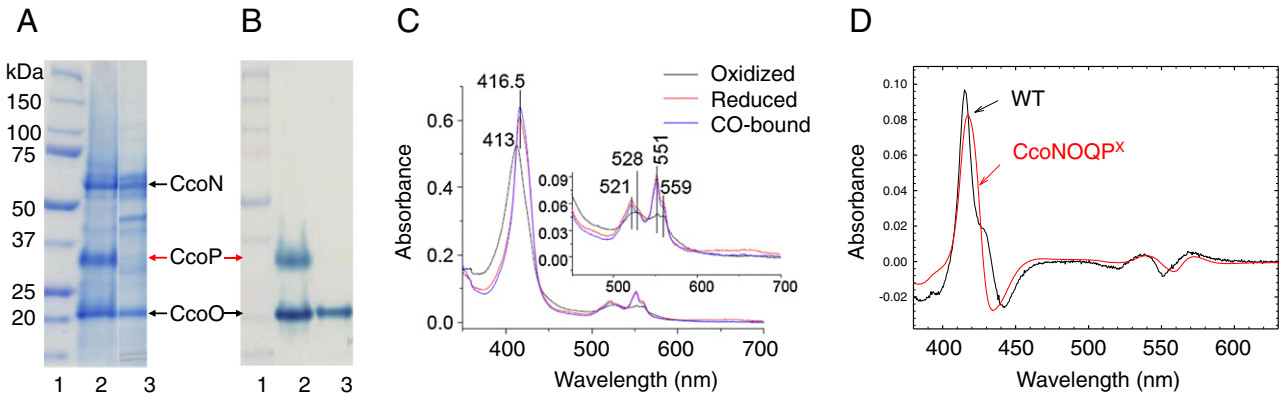

Fig. 2. Heme analysis of the wild type cytochrome *cbb*$_3$ and the truncated CcoNOQP^X (A) SDS-PAGE gel stained with Coomassie Brilliant Blue (B) SDS PAGE gel stained with 3,3′, 5,5′-tetramethyl benzidine (TMBZ) and H_2O_2 to identify a covalently bound heme *c*. Each lane contains ~10 μg of protein. In each panel, the lanes 1, 2 and 3 contains molecular weight markers, the wild type, and the truncated CcoNOQP^X enzymes, respectively (C) UV–visible spectra of the truncated CcoNOQP^X, showing the air-oxidized, dithionite-reduced and dithionite-reduced plus CO forms. The inset shows the enlarged spectra in the α- and β-band region. The buffer used was 50 mM sodium phosphate, 100 mM NaCl and 0.05% DDM at pH 8.0. (D) UV–visible spectra of the dithionite-reduced CO-bound minus dithionite-reduced form of the truncated CcoNOQP^X compared to the wild type. Experimental conditions: 50 mM Hepes, 50 mM KCl, 0.03% DDM, 3 μM PMS, 3 mM ascorbate, ~100 μM dithionite and 1 mM CO at pH 7.4 and 298 K.

to the active site in the truncated CcoNOQP^X is the same used by the wild type enzyme.

The E49A mutant has a shifted pH-dependence of the TMPD oxidase activity (Fig. 4), with a maximum at about pH 7.4, whereas the activity of the wild type enzyme increases at lower pH values. The pH-dependence of the activity of the truncated enzyme is similar to that of the wild type, consistent with the truncated enzyme using the same proton delivery channel as the wild type.

The delivery of protons to the active site of the enzyme through the K^C-channel leads to the expectation that the truncated cytochrome *cbb*$_3$ should generate a voltage across the membrane during catalytic turnover. This is due to the fact that electrons are provided from the periplasmic side of the membrane (from TMPD via CcoO for the truncated enzyme) whereas protons are from the opposite side of the membrane, corresponding to the cytoplasm in vivo. This prediction was tested by measuring the TMPD oxidase activity of the wild type and truncated enzymes reconstituted in proteoliposomes. This should generate a transmembrane voltage (proton motive force) that will act to slow the rate of enzyme catalysis. Addition of a protonophore will collapse the proton motive force and, therefore, result in increased enzymatic activity. The activities of the enzymes in proteoliposomes were measured in the absence (controlled activity) or presence (uncontrolled activity) of a protonophore. The steady state activity increased in the presence of a protonophore for both the wild type and truncated enzymes (Table 2). The ratio of uncontrolled/controlled activity, known as the respiratory control ratio (RCR), is about 4 for the wild type enzyme and 2.7 for the CcoNOQP^X enzyme. Hence, catalysis by the truncated enzyme generates a charge separation across the bilayer.

3.4. Expression of the hydrophilic domain of CcoP and its efficiency as an electron donor to the truncated cytochrome *cbb*$_3$

Using the same protocol used for the expression of *V. cholerae* cytochrome c_4 [26], the hydrophilic domain of CcoP (denoted by CcoP^{sol}) was expressed (Fig. 5). CcoP^{sol} was reduced and tested as a reductant for steady state activity with the truncated cytochrome *cbb*$_3$. No oxygen reductase activity was observed using concentrations of CcoP^{sol} up to 50 μM (Fig. 6), suggesting that the binding affinity of the hydrophilic domain of CcoP is very low and the majority of the interaction free energy between CcoP and the CcoNO complex must be mediated through the membrane domains. Furthermore, the truncated enzyme exhibits no activity using the natural electron donor, the reduced cytochrome c_4, either in the presence or the absence of CcoP^{sol} (Fig. 6). Not surprisingly, the periplasmic domain of CcoP is necessary for the functional interaction of cytochrome c_4.

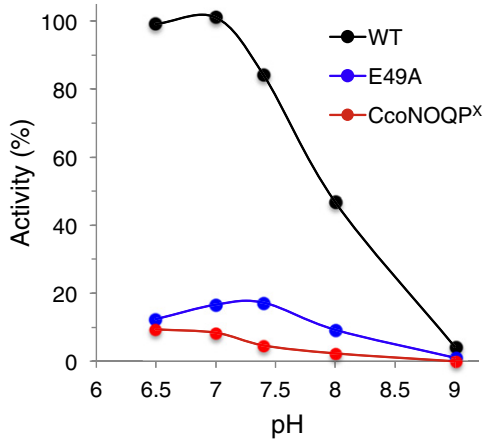

Fig. 4. pH dependence of the steady-state oxygen reductase activity of the wild type cytochrome *cbb*$_3$, the truncated CcoNOQP^X variant and the E49^{III}A mutant of the full length enzyme. The assays, using TMPD as the electron donor, were performed as described in the text.

Table 2
Comparison of O_2 reduction activities and respiratory control ratio (RCR) of the wild type and mutant enzymes before and after reconstitution into phospholipid vesicles.

cbb$_3$	Activity (e^-/s/*cbb*$_3$)			
	In detergent	In vesicles		
		Controlled	Uncontrolled	RCR
WT	198 ± 8 (100%)	17	62	3.9
CcoNOQP^{89X} (his^I)	18 ± 2 (9%)	8	21	2.7
E49^{III}A	20 ± 2 (10%)	12	24	2.2

3.5. Spectroscopic characterization of the hemes

After verifying the normal subunit assembly and stability of the native and truncated enzymes, the hemes of the enzymes were examined by spectroscopic analysis. Fig. 2C shows the UV–visible spectra of the air-oxidized, the dithionite-reduced and CO-bound forms of the truncated enzyme. There is a small but reproducible red shift in the Soret band of the oxidized form of the truncated enzyme from 411 nm to 413 nm compared to the wild type. This is likely due to the absence of the two heme *c*'s from CcoP. The reduced form of the truncated enzyme shows smaller 550/560 ratio compared to the wild type, also consistent with the lack of the heme *c* components in CcoP (Fig. 2C). Fig. 2D shows the UV–visible spectra of CO-bound minus dithionite-reduced form of the truncated enzyme along with wild type. There are distinct differences between the wild type and the truncated enzyme in the absorption of the reduced CO derivative. The observed changes at 559 nm but not at 551 nm in the truncated enzyme compared to the wild type suggest CO binding to the truncated enzyme at the heme b_3 active site but not to the remaining heme *c*. The difference between these spectra is accounted for by realizing that in the wild type *cbb*$_3$ from *P. stutzeri*, CO has been previously shown to bind to both heme b_3 and to one of the heme *c* components of CcoP [27,28]. Since the truncated enzyme lacks the heme *c* components of CcoP, it is not surprising that the spectroscopic features of CO binding to heme *c* are absent in the CO-bound *minus* reduced difference spectrum of the truncated enzyme.

The hemes were further characterized by resonance Raman spectroscopy. The oxidized truncated enzyme is substantially photoreduced when exposed to the laser beam during resonance Raman measurements to a much greater extent than the oxidized wild type enzyme. This is shown by the presence of a large contribution at 1363 cm^{-1} in the spectrum from the truncated enzyme (Spectrum a in Fig. 7B) compared to the weaker contribution in the wild type enzyme (Spectrum b in Fig. 7B). The 1362–1363 cm^{-1} band shown in Spectra e and f in Fig. 7B originates from the fraction of the enzyme that has been reduced. For both the wild type and truncated enzymes, subtraction of the appropriate amount of the spectrum of the reduced enzyme from that of the oxidized enzyme so as to eliminate the band at 1363 cm^{-1} reveals nearly identical spectra corresponding to that of the fully oxidized enzymes (Spectra c and d in Fig. 7B).

Spectra e and f in Fig. 7A show the low frequency spectra of the reduced enzymes. The 676 cm^{-1} line is assigned to heme *b* in the reduced and oxidized spectra and the lines at 686 and 694 cm^{-1} are assigned to heme *c* in the reduced and oxidized spectra, respectively. The band at 686 cm^{-1} is stronger in the spectrum of the reduced wild type enzyme (Spectrum f versus Spectrum e) due to the presence of the two additional heme *c* units. The absence of significant intensity from the 694 cm^{-1} line of oxidized heme *c* in the truncated enzyme (spectrum a) and the relative weakness of the heme *b* line at 676 cm^{-1}, indicate that heme *c* and heme *b* were both partially reduced. The greater photoreduction in the truncated enzyme may indicate a higher redox potential of the remaining heme *c* in CcoO, consistent with the slower oxidation of heme *c*

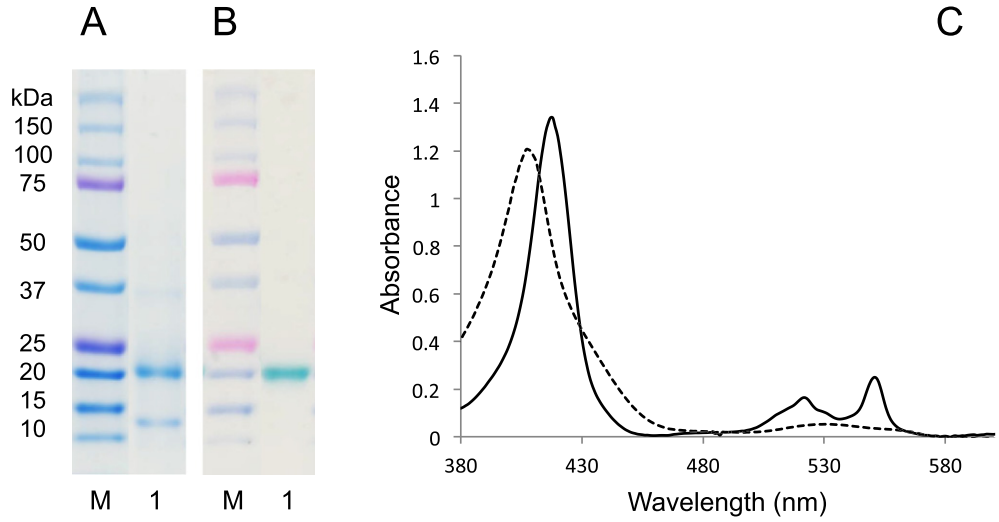

Fig. 5. Characteristics of the purified $CcoP^{sol}$. (A) SDS-PAGE gel stained with Coomassie Brilliant Blue (B): SDS PAGE gel stained with 3,3′,5,5′-tetramethyl benzidine (TMBZ) and H_2O_2 to identify a covalently bound heme *c*. Lane assignment: M, molecular weight markers; Lane 1, $CcoP^{sol}$ (C) UV–visible spectra of the ferricyanide-oxidized (dotted line) and dithionite-reduced (solid line) forms of $CcoP^{sol}$ from *V. cholerae*. The buffer used was 50 mM sodium phosphate and 100 mM NaCl at pH 8.0.

observed in the single-turnover experiments with the truncated enzyme (see Fig. 9A and C).

In addition to vibrational modes of the porphyrin macrocycles in the resonance Raman bands in the 200–800 cm^{-1} range, modes associated with Fe-ligand motions along the axis normal to the heme are also present. The CO adducts of heme proteins exhibit Fe–C–O vibrations in the 400–600 cm^{-1} region. Spectra g and h show the CO-bound forms of the dithionite-reduced enzymes in Fig. 7A and B, for the low- and high-frequency regions, respectively. In order to determine the spectra of the isolated components we have subtracted the spectra of the dithionite-reduced enzyme from those of the CO-bound, dithionite-reduced forms (Fig. 7C). Note that in the truncated enzyme, if CO only coordinates to the heme b_3 moiety, this should represent $c^{2+}b^{2+}b_3$-CO *minus* $c^{2+}b^{2+}b_3^{2+}$ (5C), where the b_3^{2+} (5C) designates the five-coordinate reduced heme b_3. The contributions from the reduced heme c^{2+} and heme b^{2+} cancel out of the difference spectra leaving a spectrum of b_3-CO *minus* b_3^{2+}(5C) but the b_3^{2+}(5C) makes no contribution to the difference spectrum as it is not enhanced with the 413.1 nm excitation. This results in spectrum c in Fig. 7C which we assign as that of pure b_3-CO. The difference spectra of the wild type enzyme (Spectrum a in Fig. 7C), which should be represented as $c^{2+}c^{2+}c^{2+}b^{2+}b_3$-CO *minus* $c^{2+}c^{2+}c^{2+}b^{2+}b_3^{2+}$ (5C), are quite different from the spectra of the truncated enzyme. This is due to CO binding to the heme *c* moieties of CcoP, consistent with the optical absorption data (Fig. 2D) and the data reported previously [27,28]. By subtracting the Spectrum c, the b_3-CO spectrum, from Spectrum a, we obtained Spectrum b, which we assign as the pure spectrum of heme c^{2+}-CO. This fully accounts for the observed spectroscopic differences between spectra a and c in Fig. 7C.

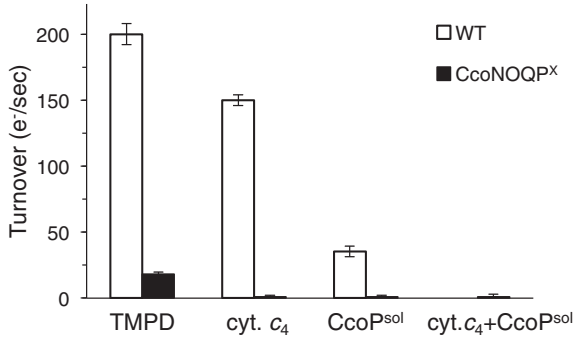

Fig. 6. Comparison of the steady-state oxygen reductase activity of the wild type cytochrome cbb_3 and the $CcoNOQP^X$ on various substrates. The enzyme activity of the truncated cbb_3 was compared to that of wild type cbb_3 on various substrates, 0.5 mM TMPD, 50 μM cytochrome c_4 and 50 μM $CcoP^{Sol}$. Experimental conditions: 50 mM sodium phosphate, 100 mM NaCl, 20 mM ascorbate and 0.05% DDM at pH 6.5 and 25 °C.

3.6. CO recombination kinetics

One test of the integrity of the heme b_3/Cu_B active site of the truncated enzyme is to determine the kinetics of recombination of CO following photolysis of CO bound to the active site of the fully reduced enzyme. Monitoring the photolysis/rebinding process at 430 nm includes CO binding to heme b_3 component of the enzyme. Fig. 8 shows that the wild type and truncated variations of the dithionite-reduced enzyme rebind to CO to a similar extent and with similar kinetics. The rate of CO recombination to heme b_3 (seen as the phase with positive amplitude on the millisecond time-scale in the figure) is the same for the wild type and the truncated variants; ~450 s^{-1} (Fig. 8A) suggesting that the truncation does not greatly perturb the rate of CO rebinding to the active site after being photolytically expelled into solution. The results indicate no substantial conformational change around the active site due to the truncation.

The CO recombination kinetics data were complicated by the presence of a second component (the rapid phase with negative amplitude in Fig. 8A). This has been previously observed with the wild type enzymes from both *P. stutzeri* and *R. sphaeroides* and shown to be due to CO rebinding to one of the heme *c* components of CcoP [27,28]. The surprising presence of the second kinetic component of CO recombination in the truncated enzyme (Fig. 8A and B) cannot be due to flash-induced dissociation of CO from the remaining heme *c* in CcoO, since the resonance Raman spectroscopy (Fig. 7C) and the UV–visible spectroscopy (Fig. 2D) show no evidence of CO binding to heme *c*. This kinetic feature is instead likely due to photodissociation of a labile axial ligand from heme *c* in CcoO, which is followed by either rebinding of the endogenous ligand or CO. Flash-induced dissociation of intrinsic ligands and competition with extrinsic ligand (CO, O_2) binding has been reported for other heme proteins [29–31]. The details of the origin of the rapid CO-binding phase in both wild type and truncated cbb_3 will be investigated further separately as it is out of the scope of this study.

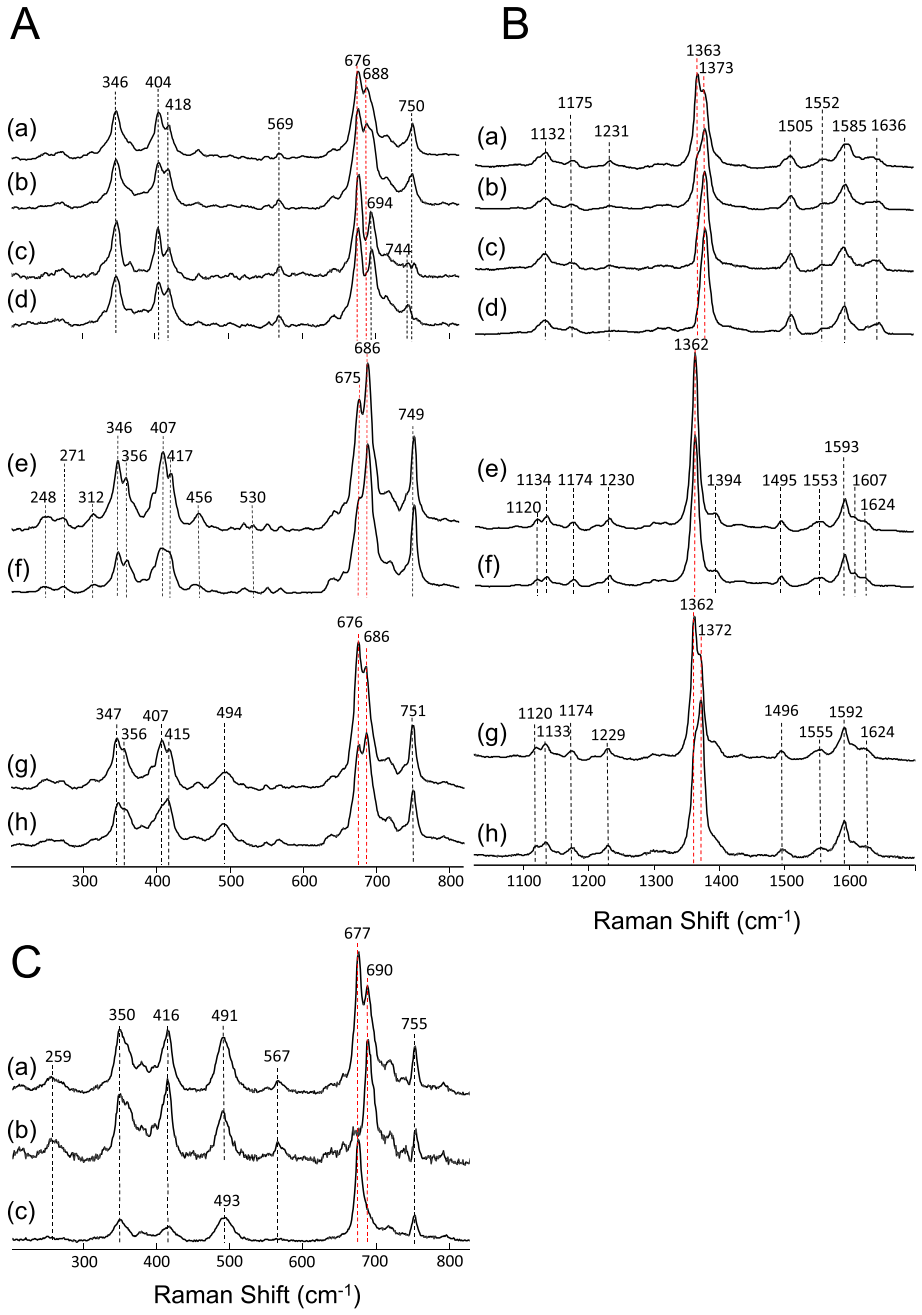

Fig. 7. Resonance Raman spectra of the oxidized (a), reduced (e) and reduced CO-bound (g) truncated enzyme, CcoNOQP^{X}, compared to those of the wild type cytochrome *cbb*$_3$ (Spectra b, f and h) in the low frequency region (A) and the high frequency region (B). Spectra c and d are the difference spectra with respect to the reduced forms of the truncated enzyme (e) and the wild type (f), respectively. (C) Resonance Raman difference spectrum (Spectrum a) of the CO-bound wild type enzyme minus its reduced form, compared to the difference spectrum (Spectrum c) of the CO-bound truncated enzyme minus its reduced form. The reduced five-coordinate heme b_3^{2+}(5C) is absent from the difference spectra because it is not enhanced with the 413.1 nm excitation and the reduced hemes *c* and the low spin heme *b* cancel out in the a and c difference spectra leaving only the spectra of the CO-bound species, which are assigned as the heme b_3-CO adduct in Spectrum c but in Spectrum a in addition to the heme b_3-CO another species is present. When the heme b_3-CO spectrum (Spectrum c) is subtracted from Spectrum a, Spectrum b is formed, which is assigned as the spectrum of a heme *c*-CO species. The laser power at the samples was ~7 mW for the oxidized and reduced forms and ~1.5 mW for the CO adducts.

3.7. Single-turnover reaction of the fully reduced enzyme with O_2

To further evaluate the properties of the truncated cytochrome *cbb*$_3$, the kinetics of the reaction of the fully reduced enzyme with O_2 was studied using the flow-flash technique. Note that the fully reduced wild type *cbb*$_3$ contains six available electrons, whereas the truncated enzyme contains four, so we expect different end products of the reaction. The end product in the wild type *cbb*$_3$ is not fully understood (see Ref. [37]), but is presumed to be a partly re-reduced intermediate. In this experiment, the CO-adduct of the fully reduced enzyme is rapidly mixed with O_2 saturated buffer and then, prior to thermal dissociation of CO, the CO is expelled from the active site by photolysis. This allows O_2 to bind to the active site, where it is reduced and the hemes are oxidized. Heme *b* is monitored at 430 nm and 560 nm whereas heme *c* is monitored at 420 nm and 550 nm. The results are shown in Fig. 9.

For the wild type enzyme, the results show that both hemes *b* and hemes *c* are oxidized in a single phase with time constant $\tau \approx 0.3$ ms ($k \approx 3300\ s^{-1}$) [25]. This is shown for both hemes *b* (Fig. 9B and

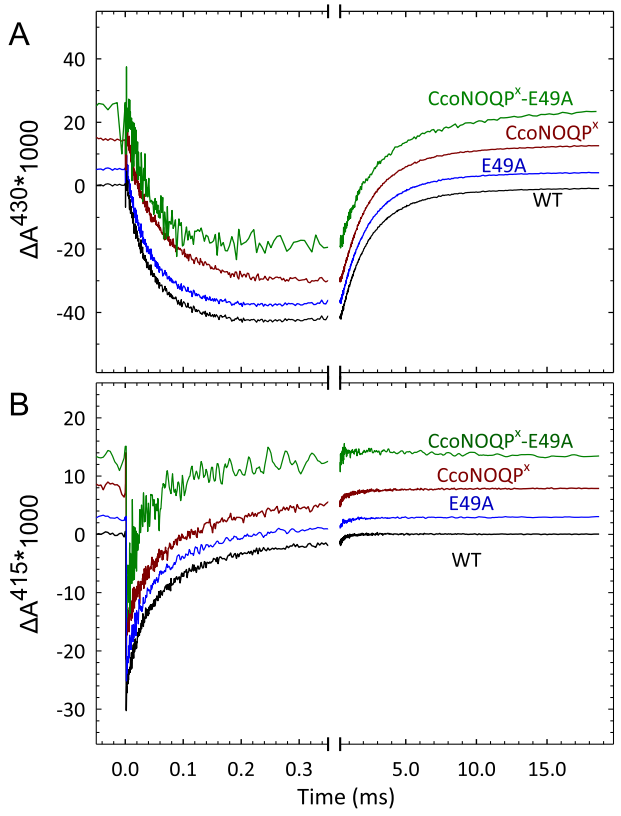

Fig. 8. CO-recombination kinetics following flash photolysis of the fully reduced wild type cytochrome cbb_3, the E49^{III}A, CcoNOQP^X and CcoNOQP^X-E49^{III}A mutants, monitored at 430 nm (A) and at 415 nm (B). (A) CO rebinding to hemes *c* and b_3 is monitored at 430 nm where both processes contribute. The rapid decrease and subsequent slow increase in absorbance correspond to CO recombination to the heme *c* and to the heme *b* components of the enzyme, respectively. (B) CO rebinding monitored at 415 nm mostly shows CO binding to a heme *c* component. Experimental conditions: 5 μM enzyme, 50 mM Hepes, 50 mM KCl, 0.03% DDM, 3 μM PMS, 3 mM ascorbate, ~100 μM dithionite and 1 mM CO at pH 7.4 and 298 K. The traces have been normalized to the same absorbance change at 0.3 ms and then spaced for better comparison. A laser artifact at t = 0 has been truncated for clarity.

D) and hemes *c* (Fig. 9A and C). The rate of oxidation of the hemes *b* in the truncated enzyme is similar to that of the wild type, $\tau \approx 0.3$ ms [25] (Fig. 9D), but the heme *c* component of the truncated enzyme is more slowly oxidized, with a time constant of $\tau \approx 1$ ms ($k \approx 1000\ s^{-1}$) (Fig. 9C + inset). The amplitude of the $\tau \approx 1$ ms phase is significantly smaller for the truncated enzyme at 420 nm and 550 nm than for the $\tau \approx 0.3$ ms in wild type, consistent with only one instead of two or three hemes *c* oxidizing.

4. Discussion

The current work definitively shows that the final assembly of cytochrome cbb_3, which is the addition of the CcoP subunit to the pre-assembled CcoNO "core" [15,18], does not require the hydrophilic diheme domain of CcoP. The first 88 amino acids of CcoP from the *V. cholerae* enzyme are sufficient for the final assembly. These data complement the previous observation that the transmembrane portion of the assembly factor CcoH is required for the interaction with CcoQP and plays a critical part in the postulated stepwise assembly of the active enzyme [22,23]. The stepwise model of assembly proposes that 1) the pre-assembled CcoNO and CcoQP subcomplexes each bind to and are stabilized by the CcoH assembly protein, forming CcoNOH and CcoQPH, and then 2) the two sub-complexes are brought together initially by interactions between the CcoH subunits in each sub-complex, forming CcoNO$(H)_2$QP. Loss of CcoH, possibly during purification, yields the final CcoNOQP active enzyme. The current results are also consistent with data from the Daldal laboratory [32] showing that the CcoN subunit could be assembled even in the absence of a fully functional cytochrome *c* maturation process and is independent of the *c*-type cytochromes.

Remarkably, the truncated CcoNOQP^X cytochrome cbb_3 is expressed in amounts similar to the wild type enzyme, is as stable as the wild type after purification, and retains about 9% of the steady state oxygen reductase activity of the wild type enzyme using TMPD as the electron donor (Table 1, Fig. 4). The absence of the hydrophilic domain of CcoP eliminates the docking site for the physiological electron donor, reduced cytochrome c_4, which therefore does not act as a reductant for the truncated enzyme (Fig. 6). Furthermore, the one remaining cytochrome *c* in

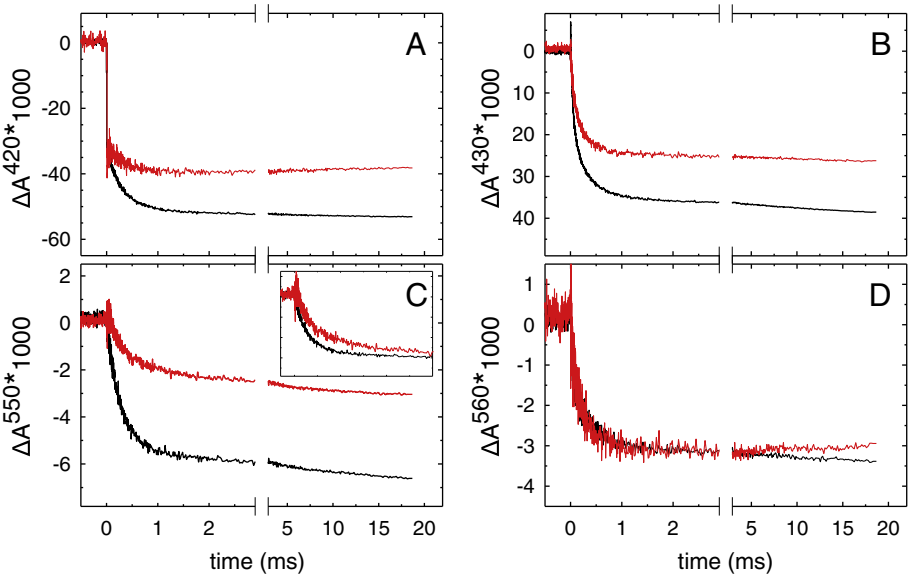

Fig. 9. Absorbance changes monitoring the reaction of O_2 with the fully reduced wild type cytochrome cbb_3 and the CcoNOQP^X variant. The absorbance changes were monitored at (A) 420 nm, (B) 430 nm, (C) 550 nm and (D) 560 nm. The absorbance decrease at 420 nm (A) and 550 nm (C) is associated with the oxidation of heme *c*, while the absorbance decrease at 430 nm (B) and 560 nm (D) is mainly due to the oxidation of low spin heme *b*. The inset in C shows the first 3 ms of the changes at 550 nm with the amplitudes arbitrarily normalized in order to emphasize the difference in rate constant. The solutions contained 1 to 2 μM of cytochrome cbb_3, 50 mM hepes, 50 mM KCl, 0.03% DDM and 1 mM O_2 at pH 7.4 and 298 K. Results with the wild type and the CcoNOQP^X variant are shown in black and in red, respectively. A laser artifact at t = 0 has been truncated for clarity.

the CcoO subunit of the truncated enzyme, is not readily accessible from solution [4] and is not rapidly reduced by the artificial electron donor TMPD. The slow steady state activity of the enzyme (about 18 s^{-1}) is likely mostly due to the slow reaction of TMPD with the truncated enzyme. This is confirmed by the rapid reaction of the fully reduced truncated enzyme with O_2, indicating that steps during the catalytic cycle other than those observed during this single-turnover experiment must be rate limiting during steady state reaction of the truncated enzyme.

Other than the slow kinetics of reduction of the enzyme during steady state catalysis due to the absence of the heme *c* components of CcoP, the truncation has only very subtle functional consequences. The remaining heme *c* associated with CcoO is more readily photoreduced (Fig. 7), and one of the axial ligands appears to be more labile upon flash photolysis (Fig. 8). It appears that the midpoint potential of this heme *c* is increased by removal of the hydrophilic domain of CcoP.

In summary, the current work shows that the hydrophobic domain of CcoP is not only essential for rapid proton uptake through the K^C-channel during catalysis, but is required for both the assembly and stability of cytochrome cbb_3. The CcoH protein requires the hydrophobic domain of CcoP for the final assembly of the enzyme. The hydrophilic domain of CcoP, in contrast, though it is required for electron transfer from the physiological electron donor, is not required either for the assembly or stability of cytochrome cbb_3.

Transparency document

The Transparency document associated with this article can be found, in the online version.

Acknowledgements

We thank Ranjani Murali and Andrew Plecki for help, and Dr. Ashtamurthy Pawate for guidance during the DLS measurements. This work was supported by grants from the National Institutes of Health grants GM098799 to D.L.R., GM086482 to S.-R.Y. and HL16101 to R.B.G., and by grants from the Swedish Research Council (621-2011-6059) and the Faculty of Science at Stockholm University to P.Ä.

References

[1] F.L. Sousa, et al., The superfamily of heme-copper oxygen reductases: types and evolutionary considerations, Biochim. Biophys. Acta Bioenerg. 1817 (4) (2012) 629–637.
[2] V. Rauhamäki, D.A. Bloch, M. Wikström, Mechanistic stoichiometry of proton translocation by cytochrome cbb_3, Proc. Natl. Acad. Sci. 109 (19) (2012) 7286–7291.
[3] H. Han, et al., Adaptation of aerobic respiration to low O_2 environments, Proc. Natl. Acad. Sci. U. S. A. 108 (34) (2011) 14109–14114.
[4] S. Buschmann, et al., The structure of cbb_3 cytochrome oxidase provides insights into proton pumping, Science 329 (5989) (2010) 327–330.
[5] H. Xie, S. Buschmann, J.D. Langer, B. Ludwig, H. Michel, Biochemical and biophysical characterization of the two isoforms of cbb_3-type cytochrome *c* oxidase from *Pseudomonas stutzeri*, J. Bacteriol. 196 (2) (2014) 472–482.
[6] M. Toledo-Cuevas, B. Barquera, R.B. Gennis, M. Wikström, J.A. García-Horsman, The cbb_3-type cytochrome *c* oxidase from *Rhodobacter sphaeroides*, a proton-pumping heme-copper oxidase, Biochim. Biophys. Acta 1365 (1998) 421–434.
[7] H.-G. Koch, O. Hwang, F. Daldal, Isolation and characterization of *Rhodobacter capsulatus* mutants affected in cytochrome cbb_3 oxidase activity, J. Bacteriol. 180 (4) (1998) 969–978.
[8] M. Raitio, M. Wikström, An alternative cytochrome oxidase of *Paracoccus denitrificans* functions as a proton pump, Biochim. Biophys. Acta 1186 (1994) 100–106.
[9] O. Preisig, R. Zufferey, L. Thony-Meyer, C.A. Appleby, H. Hennecke, A high-affinity cbb_3-type cytochrome oxidase terminates the symbiosis-specific respiratory chain of *Bradyrhizobium japonicum*, J. Bacteriol. 178 (6) (1996) 1532–1538.
[10] M.M. Pereira, J.N. Carita, R. Anglin, M. Saraste, M. Teixeira, Heme centers of *Rhodothermus marinus* respiratory chain. Characterization of its cbb_3 oxidase, J. Bioenerg. Biomembr. 32 (2) (2000) 143–152.
[11] J. Hemp, C. Christian, B. Barquera, R.B. Gennis, T.J. Martinez, Helix switching of a key active-site residue in the cytochrome cbb_3 oxidases, Biochemistry 44 (2005) 10766–10775.
[12] A. Peters, C. Kulajta, G. Pawlik, F. Daldal, H.-G. Koch, Stability of the cbb_3-type cytochrome oxidase requires specific CcoQ–CcoP interactions, J. Bacteriol. 190 (16) (2008) 5576–5586.
[13] J.I. Oh, S. Kaplan, Oxygen adaptation. The role of the CcoQ subunit of the cbb_3 cytochrome *c* oxidase of *Rhodobacter sphaeroides* 2.4.1, J. Biol. Chem. 277 (18) (2002) 16220–16228.
[14] J.-I. Oh, S. Kaplan, The cbb_3 terminal oxidase of *Rhodobacter sphaeroides* 2.4.1: structural and functional implications for the regulation of spectral complex formation, Biochemistry 38 (1999) 2688–2696.
[15] R. Zufferey, O. Presig, H. Hennecke, L. Thöny-Meyer, Assembly and function of the cytochrome cbb_3 oxidase subunits in *Bradyrhizobium japonicum*, J. Biol. Chem. 271 (15) (1996) 9114–9119.
[16] A.-L. Ducluzeau, S. Ouchane, W. Nitschke, The cbb_3 oxidases are an ancient innovation of the domain bacteria, Mol. Biol. Evol. 25 (6) (2008) 1158–1166.
[17] J.-W.L. de Gier, et al., Structural and functional analysis of aa_3-type and cbb_3-type cytochrome *c* oxidases of *Paracoccus denitrificans* reveals significant differences in proton-pump design, Mol. Microbiol. 20 (6) (1996) 1247–1260.
[18] C. Kulajta, J.O. Thumfart, S. Haid, F. Daldal, H.G. Koch, Multi-step assembly pathway of the cbb_3-type cytochrome *c* oxidase complex, J. Mol. Biol. 355 (5) (2006) 989–1004.
[19] J.I. Oh, S. Kaplan, Redox signaling: globalization of gene expression, EMBO J. 19 (16) (2000) 4237–4247.
[20] H.G. Koch, C. Winterstein, A.S. Saribas, J.O. Alben, F. Daldal, Roles of the ccoGHIS gene products in the biogenesis of the cbb_3-type cytochrome *c* oxidase, J. Mol. Biol. 297 (1) (2000) 49–65.
[21] O. Preisig, R. Zufferey, H. Hennecke, The *Bradyrhizobium japonicum* fixGHIS genes are required for the formation of the high-affinity cbb_3-type cytochrome oxidase, Arch. Microbiol. 165 (1996) 297–305.
[22] S. Ekici, G. Pawlik, E. Lohmeyer, H.G. Koch, F. Daldal, Biogenesis of cbb_3-type cytochrome *c* oxidase in *Rhodobacter capsulatus*, Biochim. Biophys. Acta 1817 (6) (2012) 898–910.
[23] G. Pawlik, et al., The putative assembly factor CcoH is stably associated with the cbb_3-type cytochrome oxidase, J. Bacteriol. 192 (24) (2010) 6378–6389.
[24] H.J. Lee, R.B. Gennis, P. Ädelroth, Entrance of the proton pathway in cbb_3-type heme-copper oxidases, Proc. Natl. Acad. Sci. 108 (43) (2011) 17661–17666.
[25] Y.O. Ahn, et al., Conformational coupling between the active site and residues within the KC-channel of the *Vibrio cholerae* cbb_3-type (C-family) oxygen reductase, Proc. Natl. Acad. Sci. U. S. A. 111 (42) (2014) E4419–E4428.
[26] H.Y. Chang, et al., The diheme cytochrome c_4 from *Vibrio cholerae* is a natural electron donor to the respiratory cbb_3 oxygen reductase, Biochemistry 49 (35) (2010) 7494–7503.
[27] Y. Huang, J. Reimann, L.M. Singh, P. Adelroth, Substrate binding and the catalytic reactions in cbb_3-type oxidases: the lipid membrane modulates ligand binding, Biochim. Biophys. Acta 1797 (6–7) (2010) 724–731.
[28] R.S. Pitcher, T. Brittain, N.J. Watmough, Complex interactions of carbon monoxide with reduced cytochrome cbb_3 oxidase from *Pseudomonas stutzeri*, Biochemistry 42 (38) (2003) 11263–11271.
[29] U. Liebl, et al., Ligand binding dynamics to the heme domain of the oxygen sensor Dos from *Escherichia coli*, Biochemistry 42 (21) (2003) 6527–6535.
[30] M.S. Hargrove, A flash photolysis method to characterize hexacoordinate hemoglobin kinetics, Biophys. J. 79 (5) (2000) 2733–2738.
[31] S. Cianetti, M. Negrerie, M.H. Vos, J.L. Martin, S.G. Kruglik, Photodissociation of heme distal methionine in ferrous cytochrome C revealed by subpicosecond time-resolved resonance Raman spectroscopy, J. Am. Chem. Soc. 126 (43) (2004) 13932–13933.
[32] S. Ekici, X. Jiang, H.G. Koch, F. Daldal, Missense Mutations in Cytochrome c Maturation Genes Provide New Insights into Rhodobacter capsulatus cbb3-Type Cytochrome c Oxidase Biogenesis, J. Bacteriol. 195 (2) (2013) 261–269.
[33] J. Hemp, et al., Comparative genomics and site-directed mutagenesis support the existence of only one input channel for protons in the C-family (cbb3 oxidase) of heme-copper oxygen reductases, Biochemistry 46 (35) (2007) 9963–9972.
[34] A. Jasaitis, M.I. Verkhovsky, J.E. Morgan, M.L. Verkhovskaya, M. Wikström, Assignment and charge translocation stoichiometries of the major electrogenic phases in the reaction of cytochrome *c* oxidase with dioxygen, Biochemistry 38 (1999) 2697–2706.
[35] T. Egawa, S.R. Yeh, Structural and functional properties of hemoglobins from unicellular organisms as revealed by resonance Raman spectroscopy, J. Inorg. Biochem. 99 (1) (2005) 72–96.
[36] M. Brändén, et al., On the role of the K-proton transfer pathway in cytochrome *c* oxidase, PNAS 98 (9) (2001) 5013–5018.
[37] Y. Huang, J. Reimann, H. Lepp, N. Drici, P. Adelroth, Vectorial proton transfer coupled to reduction of O_2 and NO by a heme-copper oxidase, Proc. Natl. Acad. Sci. U. S. A. 105 (51) (2008) 20257–20262.